

TELKOMNIKA, Vol.17, No.5, October 2019, pp.2595~2606

ISSN: 1693-6930, accredited First Grade by Kemenristekdikti, Decree No: 21/E/KPT/2018

DOI: 10.12928/TELKOMNIKA.v17i5.12810

■ 2595

# Adaptive control of nonlinear system based on QFT application to 3-DOF flight control system

Rounakul Islam Bobby<sup>\*1</sup>, Khaizuran Abdullah<sup>2</sup>, A. Z. Jusoh<sup>3</sup>, Nagma Parveen<sup>4</sup>,  
Md Mahmud<sup>5</sup>

Electrical and Computer Engineering, Kuliyah of Engineering and  
International Islamic University Malaysia, Gombak, Selangor, Malaysia, tel: (+603) 6196 4000

<sup>\*</sup>Corresponding author, e-mail: rounaqul2020@gmail.com<sup>1</sup>, khaizuran@iium.edu.my<sup>2</sup>,  
azamani@iium.edu.my<sup>3</sup>

## Abstract

Research on unmanned aerial vehicle (UAV) became popular because of remote flight access and cost-effective solution. 3-degree of freedom (3-DOF) unmanned helicopters is one of the popular research UAV, because of its high load carrying capacity with a smaller number of motor and requirement of forethought motor control dynamics. Various control algorithms are investigated and designed for the motion control of the 3DOF helicopter. Three-degree-of-freedom helicopter model configuration presents the same advantages of 3-DOF helicopters along with increased payload capacity, increase stability in hover, manoeuvrability and reduced mechanical complexity. Numerous research institutes have chosen the three-degree-of-freedom as an ideal platform to develop intelligent controllers. In this research paper, we discussed about a hybrid controller that combined with Adaptive and Quantitative Feedback theory (QFT) controller for the 3-DOF helicopter model. Though research on Adaptive and QFT controller are not a new subject, the first successful single Adaptive aircraft flight control systems have been designed for the U.S. Air Force in Wright Laboratories unmanned research vehicle, Lambda [1]. Previously researcher focused on structured uncertainties associated with controller for the flight conditions theoretically. The development of simulationbased design on flight control system response, opened a new dimension for researcher to design physical flight controller for plant parameter uncertainties. At the beginning, our research was to investigate the possibility of developing the QFT combined with Adaptive controller to control a single pitch angle that meets flying quality conditions of automatic flight control. Finally, we successfully designed the hybrid controller that is QFT based adaptive controller for all the three angles.

**Keywords:** 3-degree of freedom (3-DOF), adaptive controller, hybride controller, quantitative feedback theory (QFT), UAV

Copyright © 2019 Universitas Ahmad Dahlan. All rights reserved.

## 1. Introduction

Control theory is an interdisciplinary subdivision in the field of engineering and mathematics, which deals with the behaviours of systems' inputs, and how their behaviour is changed by feedback. The objective of each and every research on control theory is to control a dynamic system and resulting a favourite control signals or voltage as reference point. Reference point may be a fixed or changeable. To continue this procedure a controller is designed based on the control theory and it monitors the output and makes comparison with the reference [1, 2]. Automatic control system is a Software for development board which based automatic controller the carries the constant (stabilization) of a controlled variable that characterizes a technical process or the altering of the variable in accordance with a given law (program control) or with a measured external process (feedback control); the change in the value of the controlled variable is effected by applying a control action to the control element of the controlled system [3]. The (1) shows a software based automatic controller expression [4]. In automatic control, the control action  $x_0(t)$  is usually function of the dynamic error that is, of the deviation  $\varepsilon(t)$  of the controlled variable  $x(t)$  from its desired value, called the set point, Control in this case is based on the feedback principle Figure 1. which is often associated with the names of Polzunov and Watt [5]. Also sometimes classed with automatic control is control where  $x_0(t)$  is generated by a compensating unit as a function of the disturbing action load on the controlled system [6, 7].

$$X_0(t): \varepsilon(t) = x_0(t) - x(t) \quad (1)$$

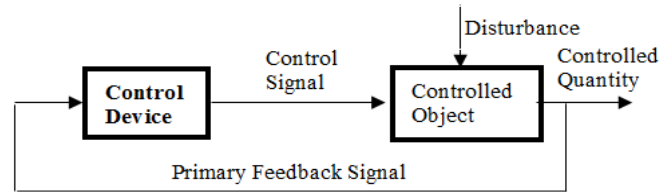


Figure 1. Deviation-  $\varepsilon(t)$  and disturbance-stimulated control based on Polzunov and Watt [5]

#### Quantitative Feedback Theory (QFT)

In control theory, quantitative feedback theory (QFT), developed by Isaac Horowitz [8, 9], is a frequency domain technique utilising the Nichols chart (NC) in order to achieve a desired robust design over a specified region of plant uncertainty. Desired time-domain responses are translated into frequency domain tolerances, which lead to bounds (or constraints) on the loop transmission function. The design process is highly transparent, allowing a designer to see what trade-offs are necessary to achieve a desired performance level. QFT is a control design methodology grounded on two ideas: i) The fact that feedback is only necessary in the presence of plant uncertainty and unknown disturbance and, ii) The notion that benefits of feedback are inextricably linked to a cost in terms of bandwidth and noise amplification. Its objective is to minimize such cost while fulfilling the specifications consequently, it recommends the use of two degree of freedom (2-DOF) structures that allow an independent adjustment of the sensitivity function and the tracking response. The feedback elements are in charge of reducing the sensitivity only to a level in which the effects of unknown disturbance and system uncertainty are acceptable. Then, the feedback element shapes the tracking response [10-12]. A QFT design technique commonly comprises these three basic steps [13]: i) Calculation of QFT bounds (robust stability, robust tracking, etc.), ii) Designing the controller (or loop shaping), iii) Evaluating the design (or possible pre-filter design).

#### Adaptive Control

Adaptive control is a specific type of control, applicable to processes with changing dynamics in normal operating conditions subjected to stochastic disturbances. The reasons for using adaptive control are, variations in process dynamics, variations in the character of disturbances, engineering efficiency. Generally, to control a process with changing dynamics is not easy [14-16]. Today two possible solutions exist for that situation: adaptive control and robust control. Adaptive control is used whenever process parameters are changing during operation and we do not know in advance what changes our process will experience. Assumption of process time invariance must be discarded. The solution has to be sought in a specific form of control where parameter estimation and regulator design will be realized on-line during normal control system operation [17]. From the Figure 2, a distributed control system is shown, used in complex hierarchical systems and that they are built upon reliable operation of lower levels such as device level (process interface) and control level (single loop control) systems. Equipment level (group control) represent even higher level where many processes are coordinated. Adaptive and robust control presented in this Figure 3, should be work in the single loop control level. Without good and reliable system operation in lower levels, there is no sense talking about higher hierarchical levels at all [18, 19].

#### Three Degree of Freedom (3-DOF)

The 3-DOF Helicopter consists of a model helicopter body, a metal base, and an aluminium frame. The helicopter has two propellers mounted in parallel, actuated by DC motors-similarly to tandem dual rotor helicopters. Figure 3 shows the 3-DOF helicopter developed by Quanser researcher group [20, 21]. The helicopter body is suspended from an instrumented joint that is mounted at the end of a long arm and is free to pitch about its centre. The other end of the arm is fastened to the base using a two degree of freedom joint. This allows the arm, and thus the helicopter, to be rotated about the vertical axis-the travel axis-as well as up and down-the elevation axis.

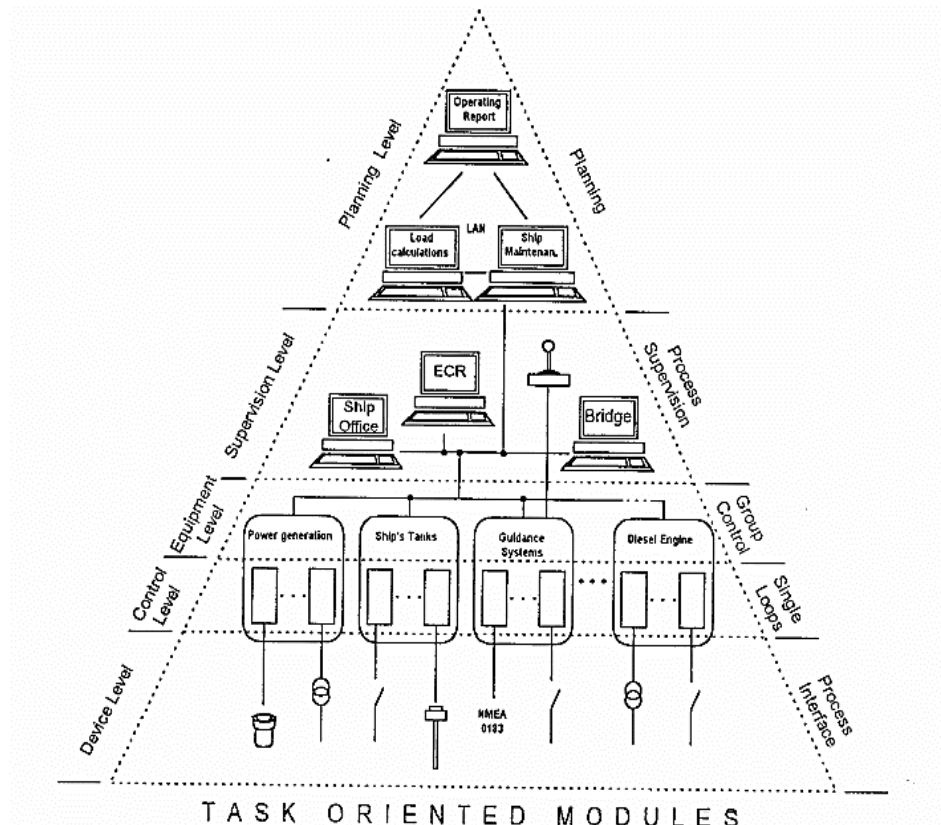


Figure 2. Distributed control system using adaptive controller [18]

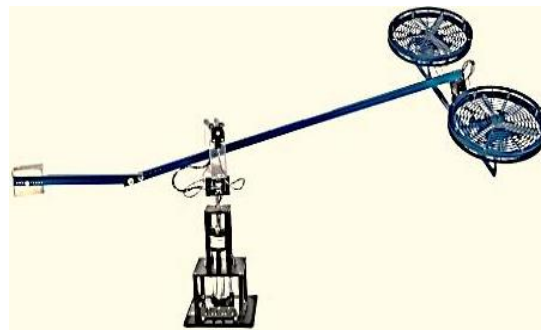


Figure 3. 3-DOF helicopter model manufactured by Quanser [21]

The other end of the arm has an adjustable counterweight that changes the effective mass of the helicopter system-making it light enough to be lifted by the thrust from the propellers. All axes are measured using high-resolution encoders to obtain precise position feedback. The slip ring mechanism on the vertical axis allows the body to rotate continuously by eliminating the need for any wires to connect the motors and encoders to the base. The front and back propellers control the movement of the helicopter [20-24]. The 3-DOF helicopter principals to control the three axis with front and back propellers, which control the movement of the helicopter. The 3-DOF Helicopter modelling conventions used are: The helicopter is horizontal when the elevation angle equals  $\varepsilon = 0$ . The travel angle increases positively, when the body rotates in the counter-clockwise (CCW) direction. The pitch angle is positive,  $p(t) > 0$ , when the front motor is higher than the back motor. The worksheet goes through the kinematics of the system. Thus, describing the front motor, back motor, helicopter body, and counterweight relative to the base coordinate system shown in Figure 4 [25-28].

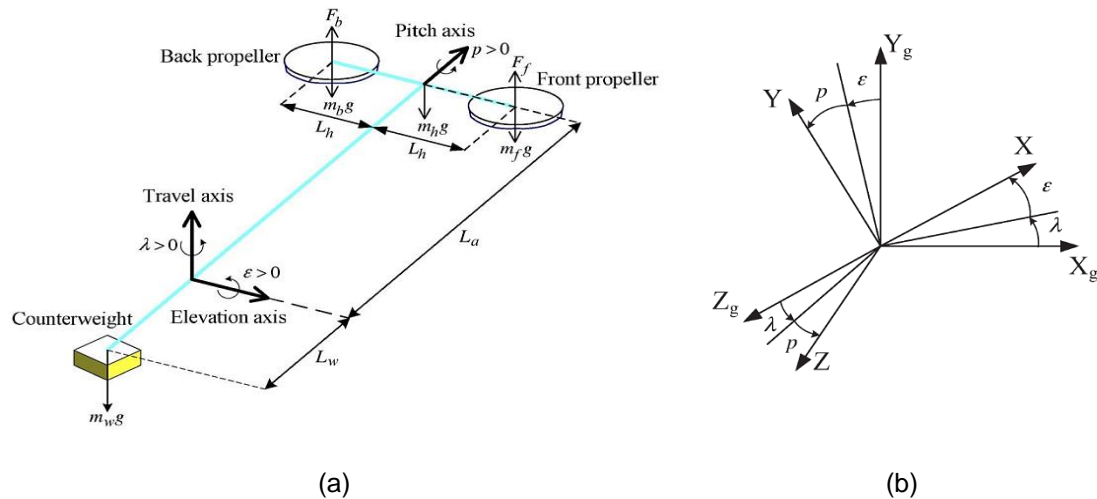


Figure 4. (a) Free-body diagram of the 3-DOF helicopter and  
(b) Spatial relations of the frames and angles [29, 30]

These resulting equations are used to find the potential energy and translational kinetic energy of the front motor, back motor, and counterweight of the system. The thrust forces acting on the elevation, pitch, and travel axes from the front and back motors are defined and made relative to the quiescent voltage or operating point.

#### 3-DOF helicopter equations

From the free-body diagram of the 3-DOF helicopter is shown in Figure 4 (a), and its spatial relations of the frames and angles are shown in Figure 4 (b). Applying the Euler–Lagrange formula, the dynamics of the helicopter can be described by differential equations. They considered the elevation motion [28-33]. The twisting moment of this axis is controlled by the composition of forces generated by the propellers.

$$J_\varepsilon \ddot{\varepsilon} = K_f L_a \cos p (F_f + F_b) - m_h g L_a \sin(\varepsilon + \alpha_0) \quad (2)$$

In (2) [29],  $\alpha_0$  is the initial angle between the helicopter arm and its base.  $J_\varepsilon$ ,  $K_f$ ,  $L_a$ ,  $F_f$  and  $F_b$  are the moment of inertia, force constant, length of body, front motor force and back motor force across to elevation angle respectively, the pitch motion is described by the following:

$$J_p \ddot{p} = K_f L_h (F_f - F_b). \quad (3)$$

In (3) [34],  $J_p$ ,  $K_f$ ,  $L_h$ ,  $F_f$  and  $F_b$  are the moment of inertia, force constant, distance of the motors from pitch axis, front motor force and back motor force across to elevation angle respectively. When the force generated by the front motor is greater than that by the back one, the helicopter body will pitch in the positive direction. The 3 DOF Helicopter model that is used in this laboratory is analogous to a tandem rotor helicopter. As described in the FBD shown in Figure 4, the pitch of the helicopter,  $p$ , is the rotation of the helicopter about a line perpendicular to the length of the body located at the centre of gravity [34-37].

## 2. Research Method

The proposed controller was simulated by MATLAB simulation process, but it is important to develop transfer function equation for the controller and observe simulation based hardware performance. For the hardware simulation process the MATLAB simulation file is needed to moderate for actual hardware, because the helicopter model can directly access through real-time QUARCH software. QUARCH is the real-time interfacing software between MATLAB software and Quanser 3-DOF helicopter's data acquisition card. MATLAB simulation block diagram can be used directly in this procedure.

## 2.1. Proposed Controller Transfer Function for 3-Dof Helicopter

The proposed design simulation architecture of the system is shown in Figure 5. The concept of hybrid adaptive with QFTcontroller is designed to adapt with its self-tunes parameters and linearly least phase systems must sacrifice to desirable feedback control benefits to obtain the desired properties in the closed-loop system. The elevation, pitch and travel motion we already developed shown as the following close loop transfer functions (4), (5) and (6): where  $\varepsilon(t)$ ,  $p(t)$  and  $\tau(t)$  are the transfer functions for elevation angle, pitch angle and travel angle respectively,  $k_f$  is the motor force-thrust constant,  $l_a$  is the distance from pivot point to motor stationary joint point and  $l_h$  is the distance from joint point or pitch axis to each motor.  $k_{ep}$  and  $k_{ed}$  are the feedback control gain of elevation axis,  $j_e$  and  $j_p$  are the moment of inertia about the elevation axis and pitch axis respectively.  $k_{pd}$  and  $k_{pp}$  are the feedback control gains of elevation axis.  $k_p$  gain control (increase  $k_p$  will increase overshoot).  $k_{rp}$  and  $k_{ri}$  are the feedback control gain of travel axis. The solved final transfer function of the system dynamics for the travel, elevation and pitch angles are shown in (7), (8) and (9).

$$\frac{\rho}{\rho_c} = \frac{\frac{K_f l_h K_{pp}}{J_p}}{s^2 + s \frac{K_f l_h K_{pd}}{J_p} + \frac{K_f l_h K_{pp}}{J_p}} \quad (4)$$

$$\rho(t) = \frac{\rho}{\rho_c} = \frac{0.6004}{s^2 + 0.9522716s + 0.6004} \quad (5)$$

$$\frac{\varepsilon}{\varepsilon_c} = \frac{\frac{K_f l_a K_{ep}}{J_e}}{s^2 + s \frac{K_f l_a K_{ed}}{J_e} + \frac{K_f l_a K_{ep}}{J_e}} \quad (6)$$

$$\varepsilon(t) = \frac{3.139167 s}{s^2 + s(0.958333) - 3.139167} \quad (7)$$

Finally,

$$\frac{\tau}{\tau_c} = \frac{\frac{-s K_p l_a K_{\tau p} + K_p l_a K_{\tau i}}{j_{\tau}}}{s^2 - s \frac{K_p l_a K_{\tau p}}{j_{\tau}} - \frac{K_p l_a K_{\tau i}}{j_{\tau}}} \quad (8)$$

$$\tau(t) = \frac{s(0.06331) - 0.13275}{s^2 + s(0.06331) + 0.13275} \quad (9)$$

## 2.2. Proposed Controller Simulation Design with 3-Dof Helicopter

For hardware simulation model, we just replace the 3-DOF helicopter block with Quanser developed hardware connected simulation block Which will automatically adjust the communication. Figure 5 shows the Quanser 3-DOF helicopter closed loop actual system block simulation. In this Figure, every block has their subsequence blocks and the desire input signal is possibly given from any one of two sources, named desired angle from program block and desire position from joystick. From the manually selector block it was selected to "program = 1", which denotes the desire angles from program block is activated manually.

The desire angle program block in Figure 5 is the angle alterable block. The sequence blocks of desire angle from program are shown in Figure 6. in this Figure the F1, F2 and F3 are the QFT filters. For the elevator angle the range was previously defined by quanser and the angle limits from  $-27^\circ$  to  $+30^\circ$ . So, initially it was given  $-27^\circ$ . For the pitch angle the constant angle is given as  $0^\circ$  to hold the straight position of the body while flying. The travel angle is different because it does not depend on elevation angle. The maximum range for the travel angle is not fixed. So, any value is suitable for taking angle. if the angle is more than  $360^\circ$  the 3-DOF helicopter will take more round and vice versa.

The second block of Figure 5 is “3-DOF heli: adaptive + QFT”, which is the same controller used for software based simulation. The controller subsequent blocks are shown in Figure 7, where the proposed adaptive with QFT controllers are also seen. Like previous the  $X$ ,  $X_1$  and  $X_2$  are the feedback input and  $X_d$  (rad) is the connection of desire angle selection.  $u(V)$  is the controller output to the helicopter model.

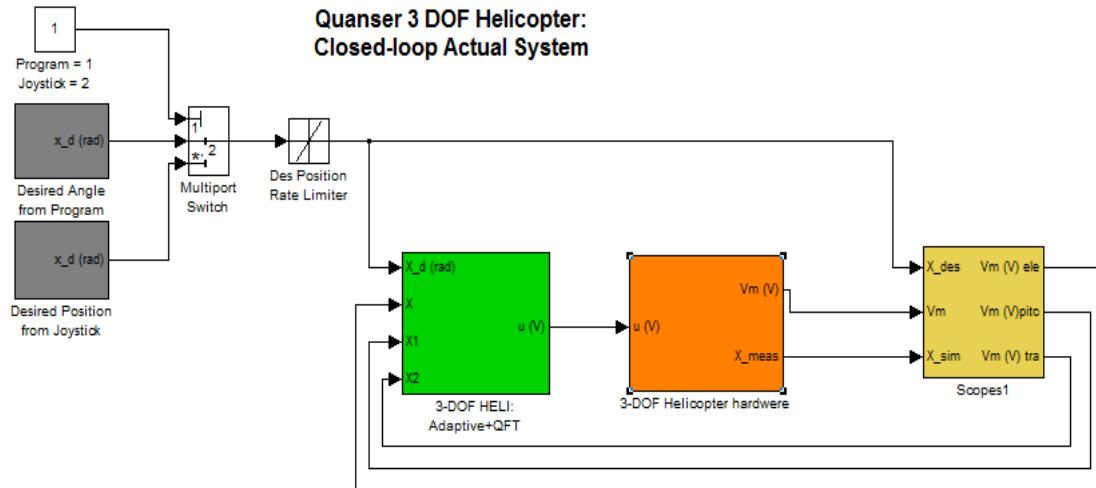


Figure 5. Quanser 3-DOF helicopter closed loop actual system block simulation

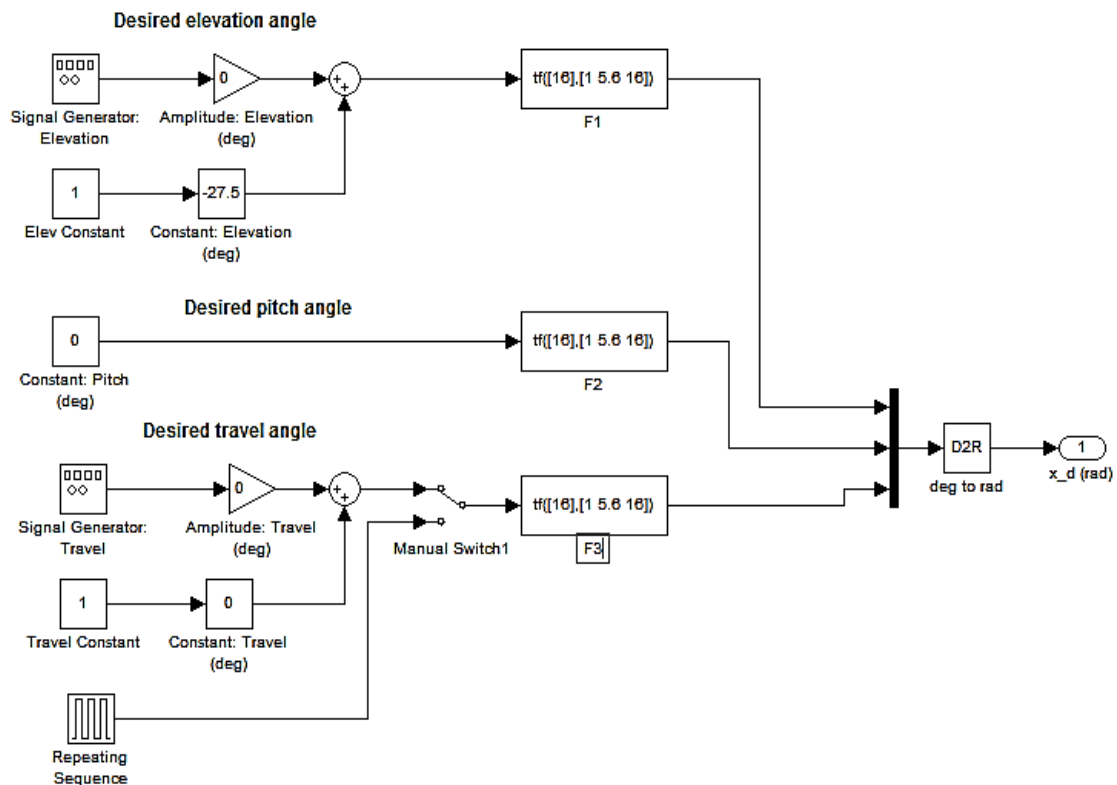


Figure 6. Desire angle from program block

The Figure 8 shows the actual helicopter hardware connection, where the “Hill rate analog” is the 3-DOF helicopter model and it is getting input signal from  $u(V)$  through limiters and

cable gain pre-compensator. The “hill read encoder” is the encoder output from data acquisition card for three angles.  $V_m$  is the motor voltage and for the two motors A0#1 and A0#2.

3-DOF Helicopter: Position Controller

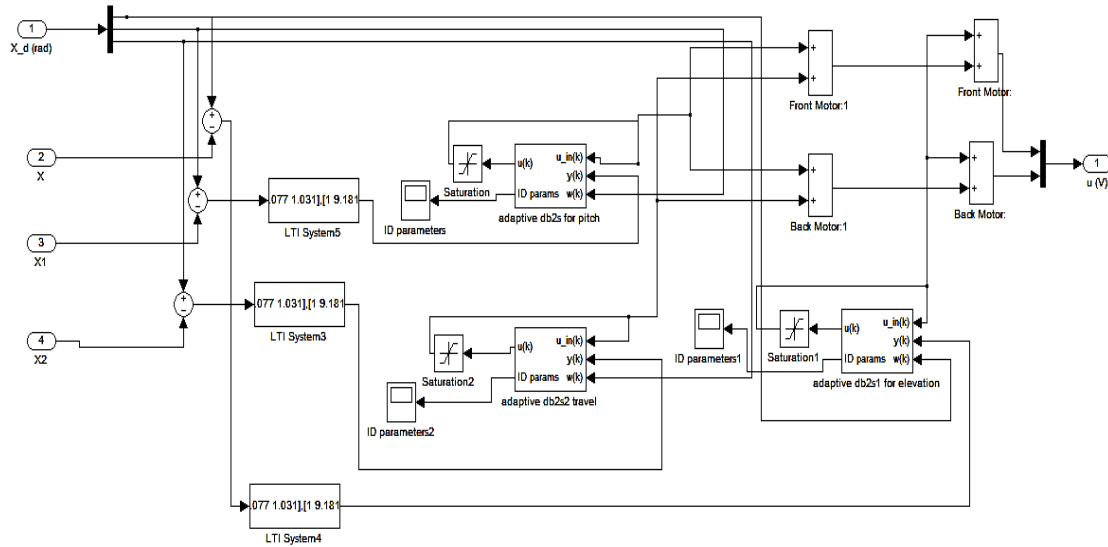


Figure 7. Proposed adaptive with QFT controllers

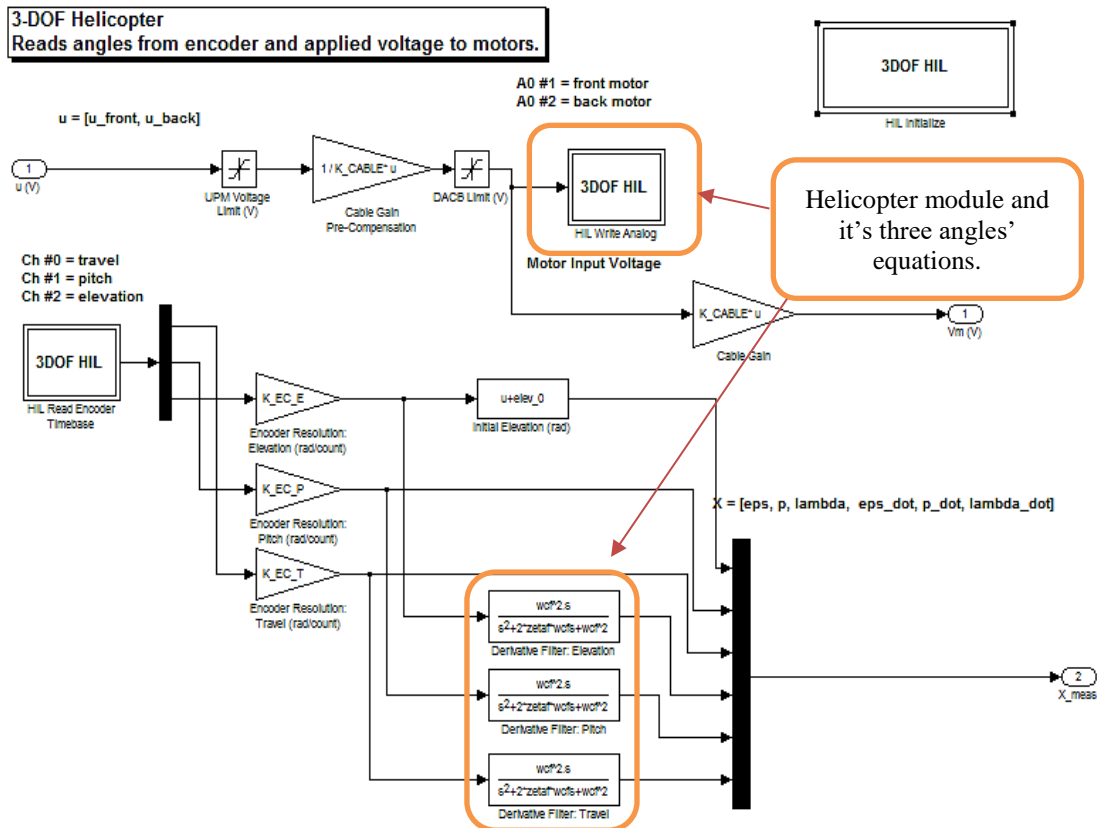


Figure 8. Actual helicopter hardware connection subsequence



To observe the performance of the controller the scope blocks were used, where every angle can be observed separately. Figure 9, shows the internal subsequence block diagram of scope block. The scope results are included in chapter five result portion.

#### Scopes

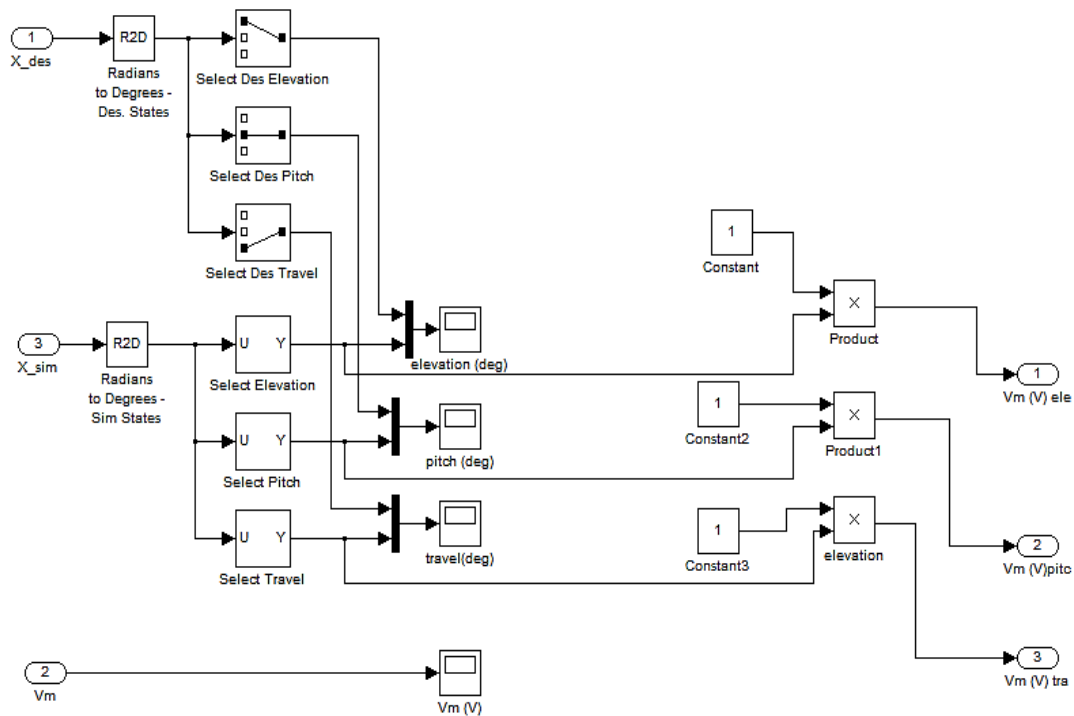


Figure 9. Internal subsequence block diagram of scope block

### 3. Results and Analysis (The Proposed Hybrid Adaptive Controller Combine with QFT)

The proposed controller is the combination of robust and adaptive controller where QFT was used as the robust controller. The simulated connection diagram of the controller has shown in Figure 6. The simulation design of proposed combined controller was tested on the predefined 3-DOF helicopter simulation model then on hardware simulation where the parameters are kept as original. The simulation outputs waveform of proposed controller is shown on Figures 10, 11 and 12. The yellow waveform is the desire angle and the red waveform is the process output result by combined controller for three angles known as elevation, pitch and travel.

#### 3.1. Travel Angle

Figure 10 is the travel angle output waveform for the proposed combined controller. From the test-bed the desire signal was given for 60° peak to peak, means 30° positive side and 30° negative side. The proposed controller successfully controlled output with a maximum overshoot of 26.67% (40.5, 10°/unit), settling time 12.5 seconds (14.5, 10 s/unit) and having zero steady state error. The output may vary from different degree but for test condition all controller was tested with the same degree of angle. All the results enclosed in Table 1.

Table 1. Adaptive + QFT controller output for travel angle

Angle output	Overshoot	Settling time(s)	Steady error	state
Proposed combined controller (Adaptive + QFT), travel angle	26.67%	12.5 seconds	00	



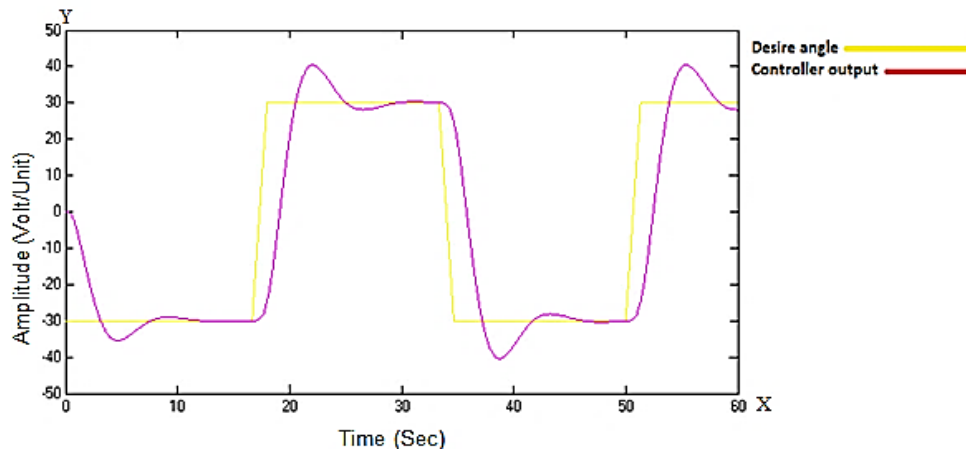


Figure 10. Response waveform of proposed combined controller with 3 DOF simulation model.

### 3.2. Elevation Angle

Figure 11, shows the elevation angle output waveform for combined controller. The desire angle amplitude was selected  $15^\circ$ pp (pic-to-pic) so  $7.5^\circ$  positive side and  $7.5^\circ$  on negative side. The output of the controller had an overshoot of 10% (9.5 V/unit), settling time 5 seconds (10 seconds/unit) and had no steady state error. The performance clearly indicates that the combined controller has higher controllability then the existing LQR controller. The results of proposed combined controller with 3 DOF simulation model for elevation angle are shown in Table 2.

Table 2. Adaptive + QFT controller output for elevation angle

Angle output	Overshoot	Settling time(s)	Steady state error
Proposed combined controller (Adaptive + QFT), elevation angle	10%	5 seconds	00

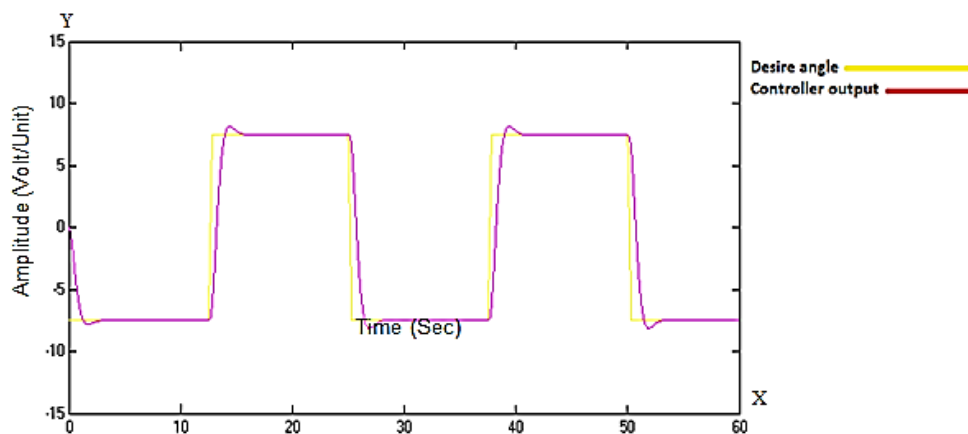


Figure 11. Response waveform of proposed combined controller with 3 DOF simulation model for elevation angle

### 3.3. Pitch Angle

The pitch angle test of 3-DOF flight control Simulink model shown in Figure 12, by using combined controller also showed good performance. The simulation model of 3-DOF helicopter model pitch angle is different from normal single test simulation. The model implies that,

the motors should keep the pitch angle to hold the helicopter model stable and always zero, predefined in chapter three section. Where the pitch has a limitation of  $20^\circ$  and the output should maintain the  $0^\circ$ , the performance of combined controller clearly indicates the maximum output is  $16.1^\circ$  and also maintaining  $0^\circ$  without steady state error. The results are shown in Table 3.

Table 3. Adaptive + QFT Controller Output for Pitch Angle

Angle output	Overshoot	Settling time(s)	Steady state error
Proposed combined controller (Adaptive + QFT) Pitch angle	00	10.8 seconds	00

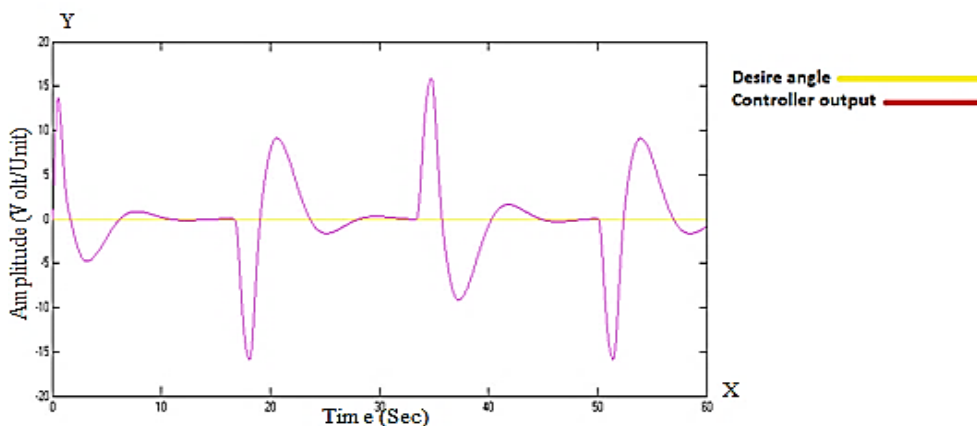


Figure 12. Response waveform of proposed combined controller with 3 DOF simulation model pitch angle

The LQR controller was re-simulated for the performance testing of proposed controller on same test bed and with the same parameter. Where the LQR controller results were recorded for comparison table. In comparison table, the three angles are shown individually, where a successful indication can obtain from the table about proposed combine controller. Generally, hybrid robust adaptive controller is better than single controller for any plant but specially some combined controller performs far better the other combined controller for specific plant model. For example, adaptive with QFT controller may perform better with 3-DOF helicopter flight control model then other controller under consideration.

#### 4. Conclusion

The method involved by combining both QFT and adaptive controllers to fully utilise the advantages and eliminates the disadvantages of the controllers. The hybrid robust adaptive controller has been tested for tracking performance via simulation. Quanser has developed simulation platform in order to evaluate the performance of the controller. The hybrid robust adaptive controller successfully has shown a better performance than single controller (individual adaptive or QFT) by reducing overshooting problem of adaptive controller and settling time of QFT controller. The combined/hybrid controller in which the actual helicopter simulation model was in the circuit. The simulation also had error minimization technique by resurrecting method of each angles and the desire angles was injected to the loop to get the desired outcome. The controller performed well and met the desired angles requirement, shown in result section. The performance of combined controller shown better performance than single controllers while performing with large uncertain range of disturbance and produced faster outcome with smaller overshoot. The outcome established that the combined controller guaranteed the specific range of uncertainty. However, the combine controller produced better process output, the unstable response was produced when range of uncertainty exceeded.

## 5. Acknowledgements

This paper was part of works conducted under the IIUM Research Initiative Grant Scheme (RIGS16-334-0498 & RIGS17-031-0606). The authors would also like to acknowledge all supports given by the IIUM Research Management Centre through the grant and RAY R&D for their research support.

## References

- [1] Lacey Jr DJ. A robust digital flight control system for an unmanned research vehicle using discrete quantitative feedback theory. Air force inst of tech wright-patterson afb oh school of engineering. 1991.
- [2] Mårtensson J, Everitt N, Hjalmarsson H. Covariance analysis in SISO linear systems identification. *Automatica*. 2017; 31(77): 82-92.
- [3] Raju M, Saikia LC, Sinha N. Automatic generation control of a multi-area system using ant lion optimizer algorithm based PID plus second order derivative controller. *International Journal of Electrical Power & Energy Systems*. 2016; 30(80): 52-63.
- [4] Filieri A, Maggio M, Angelopoulos K, D'Ippolito N, Gerostathopoulos I, Hempel AB, Hoffmann H, Jamshidi P, Kalyvianaki E, Klein C, Krikava F. *Software engineering meets control theory*. In Proceedings of the 10<sup>th</sup> International Symposium on Software Engineering for Adaptive and Self-Managing Systems. 2015: 71-82.
- [5] Novikov DA. Laws, Regularities and Principles of Control. In Cybernetics. *Springer International Publishing*. 2016: 27-38.
- [6] Scanlan JP. Technology, Culture and Development: The Experience of the Soviet Model. Routledge. 2016.
- [7] Kuzlyakina VV. Integration Processes in Engineering Education. In New Trends in Educational Activity in the Field of Mechanism and Machine Theory. *Springer, Cham*. 2014: 47-55.
- [8] Horowitz I. Invited paper Survey of quantitative feedback theory (QFT). *International Journal of Control*. 1991; 53(2): 255-291.
- [9] Bryant GF, Halikias GD. Optimal loop-shaping for systems with large parameter uncertainty via linear programming. *International Journal of Control*. 1995; 62(3): 557-568.
- [10] Horowitz I. Quantitative feedback theory. In IEEE Proceedings D (Control Theory and Applications). *IET Digital Library*. 1982; 129(6): 215-226.
- [11] Houpis CH, Rasmussen SJ, Garcia-Sanz M. Quantitative feedback theory: fundamentals and applications. CRC press. 2005.
- [12] Oby RI, Mansor H, Za'bah NF, Abidin MS, Gunawan TS, Kazmi SA. QFT Controller for Nonlinear System Application to 3-Dof Flight Control Module. *ARPN Journal of Engineering and Applied Sciences*. 2016; 11(6): 4172-4175.
- [13] Mardan M, Esfandiari M, Sepehri N. Attitude and position controller design and implementation for a quadrotor. *International Journal of Advanced Robotic Systems*. 2017; 22; 14(3): 1729881417709242.
- [14] Ahlberg JH, Nilson EN, Walsh JL. The Theory of Splines and Their Applications: Mathematics in Science and Engineering: A Series of Monographs and Textbooks. *Elsevier*. 2016.
- [15] Liu H, Li S, Li G, Wang H. Robust Adaptive Control for Fractional-order Financial Chaotic Systems with System Uncertainties and External Disturbances. *Information Technology and Control*. 2017; 46(2): 246-259.
- [16] Vu TV, Perkins D, Diaz F, Gonsoulin D, Edrington CS, El-Mezyani T. Robust adaptive droop control for DC microgrids. *Electric Power Systems Research*. 2017; 146: 95-106.
- [17] Lee ES. Quasilinearization and invariant imbedding: with applications to chemical engineering and adaptive control. Elsevier. 2016.
- [18] Sauer PW, Pai MA, Chow JH. Power System Dynamics and Stability: With Synchrophasor Measurement and Power System Toolbox. John Wiley & Sons. 2017.
- [19] Ge X, Yang F, Han QL. Distributed networked control systems: A brief overview. *Information Sciences*. 2017; 380: 117-131.
- [20] 3-DOF. HelicopterQuanserShare, [http://webcache.googleusercontent.com/search?q=cache:hbw\\_g59-2qiAJ:www.quansershare.com/Home/Search%3FtagString%3D3%2520DOF%2520Helicopter+&cd=5&hl=en&ct=clnk](http://webcache.googleusercontent.com/search?q=cache:hbw_g59-2qiAJ:www.quansershare.com/Home/Search%3FtagString%3D3%2520DOF%2520Helicopter+&cd=5&hl=en&ct=clnk).
- [21] 2 DOF helicopter and 3 dof helicopter-National Instruments. [ftp://ftp.ni.com/pub/branches/japan/academic/quanser/3\\_dof\\_helicopter\\_brochure.pdf](ftp://ftp.ni.com/pub/branches/japan/academic/quanser/3_dof_helicopter_brochure.pdf).
- [22] Zeghlache S, Benslimane T, Amardjia N, Bouguerra A. Interval Type-2 Fuzzy Sliding Mode Controller Based on Nonlinear Observer for a 3-DOF Helicopter with Uncertainties. *International Journal of Fuzzy Systems*. 2017; 19(5): 1444-1463.
- [23] Liu H, Lu G, Zhong Y. Robust LQR attitude control of a 3-DOF laboratory helicopter for aggressive maneuvers. *IEEE Transactions on Industrial Electronics*. 2013; 60(10): 4627-4636.
- [24] Liu H, Yu Y, Lu G, Zhong Y. *Robust LQR attitude control of 3DOF helicopter*. In Control Conference (CCC). 2010 29<sup>th</sup> Chinese 2010: 529-534).

- [25] Zhang L, Shi Z, Zhong Y. Attitude estimation and control of a 3-DOF lab helicopter only based on optical flow. *Advanced Robotics*. 2016; 30(8): 505-518.
- [26] Wang Y, Jiang B, Lu N, Pan J. Hybrid modeling based double-granularity fault detection and diagnosis for quadrotor helicopter. *Nonlinear Analysis: Hybrid Systems*. 2016; 21: 22-36.
- [27] Davis E, Pounds PE. Passive Position Control of a Quadrotor with Ground Effect Interaction. *IEEE Robotics and Automation Letters*. 2016; 1(1): 539-545.
- [28] Aguilar LT, Boiko I, Fridman L, Iriarte R. Introduction. In *Self-Oscillations in Dynamic Systems*. Springer International Publishing. 2015: 1-16.
- [29] Zheng B, Zhong Y. Robust attitude regulation of a 3-DOF helicopter benchmark: theory and experiments. *IEEE Transactions on Industrial Electronics*. 2011; 58(2): 660-670.
- [30] Zhang J, Cheng X, Zhu J. Control of a laboratory 3-DOF helicopter: Explicit model predictive approach. *International Journal of Control, Automation, and Systems*. 2016; 14(2): 389.
- [31] Pounds PE, Dollar AM. Stability of helicopters in compliant contact under PD-PID control. *IEEE Transactions on Robotics*. 2014; 30(6): 1472-1486.
- [32] Shan J, Liu HT, Nowotny S. Synchronised trajectory-tracking control of multiple 3-DOF experimental helicopters. *IEE Proceedings-Control Theory and Applications*. 2005; 152(6): 683-692.
- [33] De Loza AF, Rios H, Rosales A. Robust regulation for a 3-DOF helicopter via sliding-mode observation and identification. *Journal of the Franklin Institute*. 2012; 349(2): 700-718.
- [34] Zhao S, Shmaliy YS, Ahn CK, Shi P. Real-Time Optimal State Estimation of Multi-DOF Industrial Systems Using FIR Filtering. *IEEE Transactions on Industrial Informatics*. 2017; 13(3): 967-975.
- [35] Amin RU, Amin RU, Li A, Li A. Modelling and robust attitude trajectory tracking control of 3-DOF four rotor hover vehicle. *Aircraft Engineering and Aerospace Technology*. 2017; 89(1): 87-98.
- [36] Chen F, Zhang K, Jiang B, Wen C. Adaptive Sliding Mode Observer-Based Robust Fault Reconstruction for a Helicopter with Actuator Fault. *Asian Journal of Control*. 2016; 18(4): 1558-1565.
- [37] Capello E, Punta E, Fridman L. *Strategies for control, fault detection and isolation via sliding mode techniques for a 3-DOF helicopter*. In *Decision and Control (CDC)*. 2016 IEEE 55<sup>th</sup> Conference on. 2016: 6464-6469.